Immune Netw. 2024 Jun;24(3):e15
https://doi.org/10.4110/in.2024.24.e15
pISSN 1598-2629·eISSN 2092-6685

IMMUNE NETWORK

Original Article

Oxidized LDL Accelerates Cartilage Destruction and Inflammatory Chondrocyte Death in Osteoarthritis by Disrupting the TFEB-Regulated Autophagy-Lysosome Pathway

Jeong Su Lee [1,2,3,†], **Yun Hwan Kim** [4,†], **JooYeon Jhun** [1,2,3], **Hyun Sik Na** [1,2], **In Gyu Um**[1,2], **Jeong Won Choi** [1,2], **Jin Seok Woo** [1,2], **Seung Hyo Kim** [4], **Asode Ananthram Shetty** [5], **Seok Jung Kim** [4,*], **Mi-La Cho** [1,2,3,6,*]

[1]The Rheumatism Research Center, Catholic Research Institute of Medical Science, College of Medicine, The Catholic University of Korea, Seoul 06591, Korea
[2]Lab of Translational ImmunoMedicine, Catholic Research Institute of Medical Science, College of Medicine, The Catholic University of Korea, Seoul 06591, Korea
[3]Department of Biomedicine and Health Sciences, College of Medicine, The Catholic University of Korea, Seoul 06591, Korea
[4]Department of Orthopedic Surgery, Uijeongbu St. Mary's Hospital, College of Medicine, The Catholic University of Korea, Seoul 06591, Korea
[5]Institute of Medical Sciences, Faculty of Health and Wellbeing, Medway Campus of Canterbury Christ Church University, Chatham ME4 4UF, UK
[6]Department of Medical Life Sciences, College of Medicine, The Catholic University of Korea, Seoul 06591, Korea

Received: Dec 4, 2023
Revised: Mar 18, 2024
Accepted: Apr 3, 2024
Published online: Apr 12, 2024

***Correspondence to**
Mi-La Cho
The Rheumatism Research Center, Catholic Research Institute of Medical Science, College of Medicine, The Catholic University of Korea, 222 Banpo-daero, Seocho-gu, Seoul 06591, Korea.
Email: iammila@catholic.ac.kr

Seok Jung Kim
Department of Orthopedic Surgery, Uijeongbu St. Mary's Hospital, College of Medicine, The Catholic University of Korea, 222 Banpo-daero, Seocho-gu, Seoul 06591, Korea.
Email: peter@catholic.ac.kr

[†]Jeong Su Lee and Yun Hwan Kim have contributed equally to this work.

ORCID iDs
Jeong Su Lee
https://orcid.org/0009-0007-2396-7205
Yun Hwan Kim
https://orcid.org/0000-0003-1917-3465

ABSTRACT

Osteoarthritis (OA) involves cartilage degeneration, thereby causing inflammation and pain. Cardiovascular diseases, such as dyslipidemia, are risk factors for OA; however, the mechanism is unclear. We investigated the effect of dyslipidemia on the development of OA. Treatment of cartilage cells with low-density lipoprotein (LDL) enhanced abnormal autophagy but suppressed normal autophagy and reduced the activity of transcription factor EB (TFEB), which is important for the function of lysosomes. Treatment of LDL-exposed chondrocytes with rapamycin, which activates TFEB, restored normal autophagy. Also, LDL enhanced the inflammatory death of chondrocytes, an effect reversed by rapamycin. In an animal model of hyperlipidemia-associated OA, dyslipidemia accelerated the development of OA, an effect reversed by treatment with a statin, an anti-dyslipidemia drug, or rapamycin, which activates TFEB. Dyslipidemia reduced the autophagic flux and induced necroptosis in the cartilage tissue of patients with OA. The levels of triglycerides, LDL, and total cholesterol were increased in patients with OA compared to those without OA. The C-reactive protein level of patients with dyslipidemia was higher than that of those without dyslipidemia after total knee replacement arthroplasty. In conclusion, oxidized LDL, an important risk factor of dyslipidemia, inhibited the activity of TFEB and reduced the autophagic flux, thereby inducing necroptosis in chondrocytes.

Keywords: Osteoarthritis; Dyslipidemia; Low-density lipoprotein; Autophagy; Necroptosis

IMMUNE NETWORK

JooYeon Jhun
https://orcid.org/0000-0003-3953-669X
Hyun Sik Na
https://orcid.org/0000-0003-3436-2694
Jeong Won Choi
https://orcid.org/0000-0003-4299-7155
Jin Seok Woo
https://orcid.org/0000-0001-8921-2832
Seung Hyo Kim
https://orcid.org/0000-0001-6014-4477
Asode Ananthram Shetty
https://orcid.org/0000-0003-4105-7348
Seok Jung Kim
https://orcid.org/0000-0002-9116-8786
Mi-La Cho
https://orcid.org/0000-0001-5715-3989

Conflict of Interest

The authors declare no potential conflicts of interest.

Abbreviations

ApoE, apolipoprotein E; CRP, C-reactive protein; CVD, cardiovascular disease; DMM, destabilization of the medial meniscus; HDL, high-density lipoprotein; IF, immunofluorescence; IHC, immunohistochemistry; KO, knockout; LAMP1, lysosomal-associated membrane protein 1; LC3B, light chain 3B; LDL, low-density lipoprotein; LDLR, low-density lipoprotein receptor; LOX1, lectin-type oxidized low-density lipoprotein receptor 1; MIA, monosodium iodoacetate; MLKL, mixed linage kinase domain-like protein; MMP, matrix metalloproteinase; ns, not significant; OA, osteoarthritis; OARSI, Osteoarthritis Research Society International; oxLDL, oxidized low-density lipoprotein; p-, phosphorylated-; PWT, paw withdrawal threshold; RIPK3, receptor-interacting serine/threonine-protein kinase 3; SQSTM1, sequestosome-1; TC, total cholesterol; TFEB, transcription factor EB; TG, triglycerides; TKRA, total knee replacement arthroplasty; VLDL, low-density lipoprotein.

Author Contributions

Conceptualization: Lee JS, Cho ML; Data curation: Um IG, Choi JW, Woo JS, Kim SH; Formal analysis: Kim YH, Choi JW, Woo JS; Funding acquisition: Cho ML; Investigation: Lee JS, Jhun J, Na HS, Um IG; Methodology: Na HS; Project administration: Lee JS; Resources: Kim YH, Kim SH, Kim SJ; Supervision: Shetty AA, Kim SJ, Cho ML; Validation: Lee JS, Na HS; Writing - original draft: Lee JS, Kim YH, Jhun J; Writing - review & editing: Lee JS, Jhun J, Kim SJ, Cho ML.

INTRODUCTION

Osteoarthritis (OA) is a chronic joint disorder caused by an inflammatory response to cartilage, synovial membranes, and surrounding tissues, leading to joint destruction (1,2). OA causes a marked reduction in quality of life. Cartilage is composed of extracellular matrix (ECM) and chondrocytes as the main cell type. Chondrocytes maintain the function and structure of cartilage and homeostasis by synthesizing and secreting ECM (3,4). Cartilage tissue recuperates slowly and has a low ECM turnover rate (5,6). Dyslipidemia is a risk factor for aggravation of OA.

A Western diet has been linked to a variety of diseases, and weight gain can worsen arthritis (7). Dyslipidemia is a risk factor for worsening of OA. Dyslipidemia is characterized by an excessively high level of low-density lipoprotein (LDL) in the blood and is a precursor of cardiovascular disease (CVD) (8). When present in excessive amounts, LDL is oxidized to oxidized LDL (oxLDL), a key initial risk factor for CVD, which induces inflammation, decreases autophagic flux, and triggers necroptosis of endothelial cells and macrophages (5). A study on metabolic syndrome and arthritis has been published (9). LDL, high-density lipoprotein (HDL), and total cholesterol (TC) concentrations influence arthritis (9-11).

The role of oxLDL in the pathogenesis of OA is unclear. The expression of lectin-type oxidized LDL receptor 1 (LOX1) in cartilage is increased in animal models of OA and in patients with OA (12). Knockout (KO) of LOX1 suppresses OA development (13), and oxLDL inhibits proteoglycan synthesis and causes the death of chondrocytes in patients with OA (14). An increased cholesterol level in chondrocytes induces the production of catabolic factor, which aggravates OA (15,16). The oxLDL level is increased in the synovium of patients with OA, causing TNF-α-mediated apoptosis (17). oxLDL is important in the pathogenesis of OA, but the mechanism is unclear.

Autophagy is an intracellular mechanism for removing unnecessary or dysfunctional components and is important for maintaining chondrocyte function and homeostasis. Decreased autophagic flux suppresses chondrocyte function and homeostasis, which adversely affects cartilage function and exacerbates OA (18). Autophagic flux is reduced in OA, and its restoration alleviates the disease. Defects in chondrocyte autophagy lead to increased apoptosis and inflammatory death of chondrocytes, promoting the progression of OA (19,20). Therefore, it is important to investigate the roles in the pathogenesis of OA of factors that exacerbate autophagy.

We conducted a mechanistic investigation of oxLDL-induced OA by assessing the effect of oxLDL on autophagy in chondrocyte, and the clinical manifestations of oxLDL-induced OA, monosodium iodoacetate (MIA)-induced OA, and surgery-induced hyperlipidemia in apolipoprotein E (ApoE) KO mice.

MATERIALS AND METHODS

Animals

Nine-week-old male C57BL/6 mice (OrientBio, Seongnam, Korea) and ApoE-deficient ($ApoE^{-/-}$) mice (Jackson Laboratories, Bar Harbor, ME, USA) were maintained in groups of three in polycarbonate cages in a specific pathogen-free environment. Nine-week-old male $ApoE^{-/-}$ mice

were fed a western diet (based on the Research Diets #D12079B formulation) and water *ad libitum*. Nine-week-old male C57BL/6 mice had *ad libitum* access to a gamma-irradiated sterile diet (TD 2018S; Envigo, Indianapolis, IN, USA) and autoclaved reverse-osmosis water.

The animal experiments were performed in accordance with the guidelines of the Laboratory Animal Welfare Act. The Catholic Medical School Institutional Animal Care and Use Committee and Department of Laboratory Animals at the Catholic University of Korea, Songeui Campus, was accredited by the Korean Excellence Animal Laboratory Facility in accordance with the Korean Food and Drug Administration in 2017 and full accreditation by the Association for Assessment and Accreditation of Laboratory Animal Care International was acquired in 2018.

Analysis of serum lipid levels

Blood (1 mL) was obtained from mice by cardiac puncture and centrifuged at 8,000 rpm for 8 min to separate serum. The serum levels of TC (Cat. No. 03039773 190; Roche, Mannheim, Germany), HDL-cholesterol (Cat. No. 07528566 190; Roche), and LDL-cholesterol (Cat. No. 07005717 190; Roche) were measured using the Cobas C502 analyzer (Roche).

MIA-induced arthritis model

After anesthesia with 2% isoflurane, 10-wk-old male C57BL/6 and ApoE$^{-/-}$ (n=6) mice were injected intra-articularly with 20 μl of 1 mg MIA (Sigma, St. Louis, MO, USA) into the right knee using a Hamilton syringe.

Destabilization of the medial meniscus (DMM) surgery–induced OA mouse model

For OA induction, 10-wk-old male C57BL/6 mice and ApoE$^{-/-}$ mice were anesthetized with 2% isoflurane. Regarding DMM, a number 11 surgical blade was used to destabilize the medial meniscus of the right knee of the mouse. Next, the internal wound site was sutured with coated Vicryl polyglactin 910 (Ethicon, Raritan, NJ, USA). The epidermis was sutured with non-absorbable black silk suture (Ethicon). Mice with OA were randomly assigned to groups (n=6 per group). All procedures were performed under a microscope.

Assessment of pain

Joint nociception was assessed using a von Frey aesthesiometer, in an electronic version of the von Frey procedure used to evaluate mechanical sensitivity. Mice were placed on a metal mesh surface in an acrylic chamber and rested for 10 min before testing. The device was used to stimulate the plantar surface of the paw vertically. The force that induced the paw withdrawal reflex was automatically recorded in grams, and a maximum of 90 g of force was applied. All procedures and tests were performed in a blinded manner by 2 investigators.

Differentiation of primary chondrocytes from the articular cartilage of patients with OA

Patients with OA were recruited from the Department of Orthopedic Surgery at Seoul Uijeongbu St. Mary's Hospital (IRB No. UC23TISI0069). Chondrocytes were isolated from the articular cartilage of patients who underwent arthroplasty or joint replacement surgery. Cartilage was isolated using 0.5 mg/ml hyaluronidase, 5 mg/ml protease type XIV, and 2 mg/ml collagenase type V, and chondrocytes were cultured in DMEM with 10% FBS.

Histopathological analysis

We obtained joint tissue from the mice 5 wk after MIA induction and 8 wk after DMM surgery. Paraffin-embedded joint-tissue sections of 5-μm thickness were subjected to paraffin

https://doi.org/10.4110/in.2024.24.e15

removal, hydration, and dehydration, followed by Safranin O staining and mounting on slides for histopathological analysis.

Immunohistochemistry (IHC)

For mouse cartilage IHC, Abs against microtubule-associated proteins 1A/1B light chain 3B (LC3B; 1:100, Cat. No. ab48394; Abcam, Cambridge, UK), sequestosome-1 (SQSTM1/p62; 1:100, Cat. No. #5114; Cell Signaling Technologies, Danvers, MA, USA), receptor-interacting serine/threonine-protein kinase 3 (RIPK3; 1:200, Cat. No. PA5-19956; Invitrogen, Waltham, MA, USA), phosphorylated-mixed linage kinase domain-like protein S345 (p-MLKL S345; 1:250, Cat. No. ab196436; Abcam), matrix metalloproteinase 13 (MMP13; 1:300, Cat. No. ab39012; Abcam), IL-1β (1:400, Cat. No. NB600-633; Novus, Centennial, CO, USA), TNF-α (1:150, Cat. No. ab6671; Abcam), and IL-6 (1:200, Cat. No. nb600-1131; Novus) were incubated at 4°C overnight. For OA patient cartilage IHC, we used Abs against LC3B (LC3B; 1:50, Cat. No. sc-376404; Santa Cruz Biotechnology, Dallas, TX, USA), sequestosome-1 (SQSTM1/p62; 1:100, Cat. No. #5114; Cell Signaling Technologies), RIPK3 (1:200, Cat. No. PA5-19956; Invitrogen), and p-MLKL S125 (1:150, Cat. No. PA5-105677; Invitrogen). The above procedures were performed in a blinded manner by 2 investigators.

Immunofluorescence

Autophagic flux was assayed using the Premo Autophagy Tandem Sensor RFP-GFP-LC3 Kit (Cat. No. P36239, 30 particles per cell; Invitrogen). Lysosomal activity was measured using LysoSensor Green DND-189 (Cat. No. L7535, 1 μM; Invitrogen). For immunofluorescence (IF) of chondrocytes, unconjugated transcription factor EB (TFEB; Cat. No. #5114, 1:1,000; Cell Signaling Technologies) was used for primary culture, and TFEB was incubated with a donkey anti-goat Alexa Fluor 488 secondary Ab (Cat. No. A-11055, 1:200; Invitrogen), and PE-conjugated-LAMP1 (Cat. No. sc-20011 PE, 1:200; Santa Cruz Biotechnology) were cultured. Nuclei were stained with DAPI. For IF of necroptosis, unconjugated RIP3 (Cat. No. PA5-19956, 1:200; Invitrogen) was used for primary culture, and RIP3 was incubated with a goat anti-rabbit Alexa Fluor 488 secondary Ab (Cat. No. A-11008, 1:200; Invitrogen). Unconjugated p-MLKL S358 (Cat. No. ab187091, 1:50; Abcam) was used for primary culture, and p-MLKL was incubated with a goat anti-rabbit Alexa Fluor 488 secondary Ab (Cat. No. A-11008, 1:200; Invitrogen). Nuclei were stained with DAPI, and IF signals were analyzed using ZEN v. 3.2 software (Blue Edition; Zeiss, Oberkochen, Germany). For IF of joint tissues, unconjugated TFEB (Cat. No. #5114, 1:200; Cell Signaling Technologies) was used for primary culture, and TFEB was incubated with a goat anti-rabbit Alexa Fluor 488 secondary Ab (Cat. No. A-11008, 1:400; Invitrogen).

Western blotting

Chondrocytes (1.5×10^5/well) were treated with 20 μg/ml oxLDL (L34357; Invitrogen) and 10 μM rapamycin (Cat. No. S1039; Selleckchem, Houston, TX, USA) for 1 or 24 h. Proteins isolated from cells were resolved by SDS-PAGE and transferred to nitrocellulose membranes (Amersham Pharmacia Biotech, Piscataway, NJ, USA), followed by Western blotting using SNAP IDs. To visualize protein bands, we used an enhanced chemiluminescence detection kit (Thermo Fisher Scientific, Waltham, MA, USA) with Abs against LC3B (1:1,000), SQSTM1/p62 (1:1,000), phospho-p44/42 MAPK (extracellular signal-regulated kinase (Erk)1/2) Thr202/Tyr204 (pERK1/2 Thr202/Tyr204; 1:1,000, Cat. No. #4370; Cell Signaling Technologies), p44/42 MAPK (Erk1/2) (ERK1/2; 1:1,000, Cat. No. #4695; Cell Signaling Technologies), phospho-mTOR S2448 (p-mTOR S2448; 1:1,000, Cat. No. #5536; Cell Signaling Technologies), mTOR (1:1,000, Cat. No. #2983; Cell Signaling Technologies),

phospho-transcription factor EB S211 (pTFEB S211; 1:1,000, Cat. No. #37681; Cell Signaling Technologies), TFEB (1:1,000), lysosomal-associated membrane protein 1 (LAMP1; 1:2,000, Cat. No. #3243; Cell Signaling Technologies), p-MLKL Ser358 (p-MLKL S358; 1:1,000, Cat. No. CS214775; Millipore, Burlington, MA, USA), MLKL (MLKL; 1:1,000, Cat. No. CS214789; Millipore), RIP3 (1:1,000), and GAPDH (1:10,000, Cat. No. ab181602; Abcam). The primary Abs were diluted in 1% BSA in Tris-buffered saline with Tween-20 and incubated for 20 min at room temperature. The membrane was washed and incubated with the corresponding HRP-conjugated secondary Ab for 20 min at room temperature. Western blot bands were quantitatively analyzed using Fiji/ImageJ software (NIH, Bethesda, MD, USA).

Statistical analysis

The significance of between-group differences was calculated by one-way ANOVA. Two-way ANOVA was performed for assessment of the paw withdrawal threshold (PWT) and weight change. The importance of between-group differences was evaluated by the Bonferroni *post hoc* test. Numerical data were compared between groups using the Mann–Whitney test and unpaired *t*-test. Data are presented as means ± SEM. A p-value <0.05 was considered to indicate statistical significance. Statistical analysis was performed using Prism v. 9.31 software (GraphPad Software Inc., San Diego, CA, USA). General characteristics were considered as mean and SD for continuous variables and frequency percentage for categorical variables. Comparison between the 2 groups was analyzed using Independent *t*-test or χ^2 test depending on the characteristics of the variables.

RESULTS

oxLDL inhibits autophagic flux in OA chondrocytes

Impaired regulation of autophagy contributes to the development of OA. oxLDL causes autophagy dysregulation in endothelial cells and macrophages. We investigated the effect of oxLDL on the regulation of autophagy in chondrocytes. LC3B promotes the expansion and completion of autophagosomes by binding to the phagophore. p62/SQSTM1 recognizes aggregated and/or unnecessary proteins in a cell and targets them for autophagy by binding to LC3B and autophagosomes. Under normal autophagic flux, autophagosomes combine with lysosomes to degrade and recycle unnecessary proteins and p62/SQSTM1. However, if the autophagic flux is abnormal, the degradation and recycling of unnecessary proteins and p62/SQSTM1 are impaired. Western blotting showed that the p62/SQSTM1 level was higher in oxLDL-treated chondrocytes compared to the control (21,22). Rapamycin, an enhancer of autophagy, decreased the level of p62/SQSTM1 compared to oxLDL-treated chondrocytes, indicating rescue of the oxLDL-induced abnormal autophagic flux (**Fig. 1A**). To assess the autophagic flux in human OA chondrocytes, we used the Autophagy Sensor and conducted IF analysis (23). oxLDL increased the accumulation of autophagosomes (yellow GFP-RFP dots), whereas cotreatment with rapamycin reduced the number of yellow dots. Therefore, oxLDL caused dysregulation of autophagy in chondrocytes, an effect reversed by rapamycin (**Fig. 1B**).

mTOR is a kinase that regulates cellular growth, metabolism, and autophagy. mTOR inhibits the activation of TFEB, which regulates lysosome biogenesis and autophagy, by inducing its phosphorylation in the cytoplasm (24). ERK1/2 is activated by external stimuli and is involved in cell proliferation and differentiation (24,25). ERK1/2 phosphorylates TFEB and inhibits its nuclear translocation. Western blotting showed higher levels of p-mTOR, pERK1/2, and pTFEB, and a decreased level of LAMP1, in oxLDL-treated chondrocytes

 https://doi.org/10.4110/in.2024.24.e15

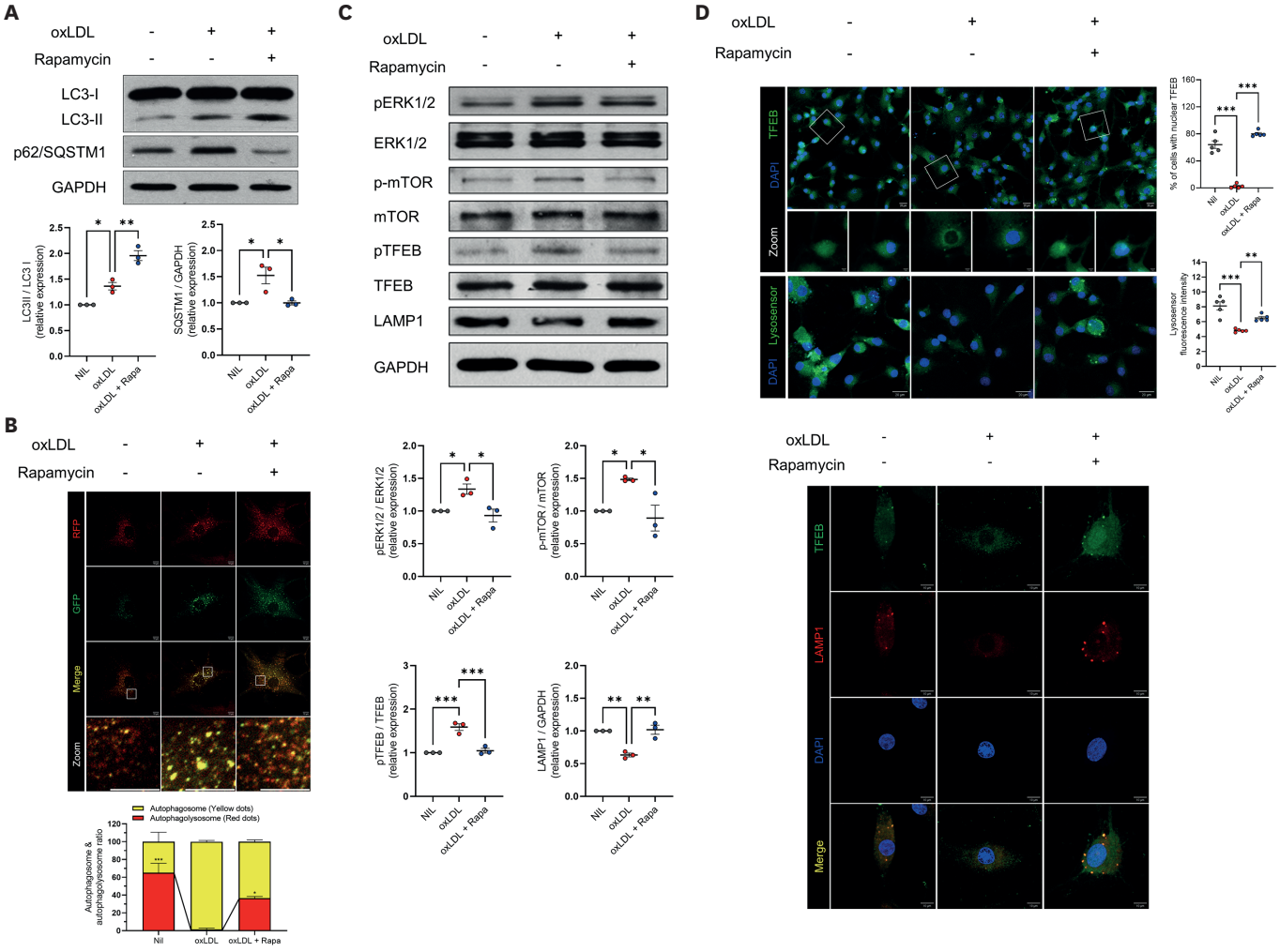

Figure 1. oxLDL inhibits autophagic flux in articular chondrocytes from the knees of patients with OA, an effect rescued by rapamycin. (A) Chondrocytes from patients with OA were stimulated with oxLDL (20 μg/ml) and rapamycin (100 nM) for 24 h, and LC3B, p62, and GAPDH levels were analyzed by western blotting. (B) Chondrocytes from patients with OA were transfected with autophagy Tandem Sensor RFP-GFP-LC3B for 48 h and stimulated with oxLDL (20 μg/ml) and rapamycin (100 nM) for 24 h. Autophagosomes (GFP-RFP, yellow dots) and autophagolysosomes (RFP dots, red) were observed by IF (magnifications ×600, ×4,800). (C) Chondrocytes from patients with OA were stimulated with oxLDL (20 μg/ml) and rapamycin (100 nM) for 1 h, and the pERK1/2, ERK/12, p-mTOR, mTOR, pTFEB, TFEB, LAMP1, and GAPDH levels were analyzed by western blotting. (D) Chondrocytes were stimulated with oxLDL (20 μg/ml) and rapamycin (100 nM) for 1 h and TFEB nuclear translocation was examined by IF (magnifications ×200, ×1,000). Lysosome activity was assessed using LysoSensor Green DND-189 (magnification ×400). TFEB (green), LAMP1 (red), and DAPI were observed by IF.
Data are mean ± SEM; statistical significance was evaluated by the Bonferroni test.
*p<0.05, **p<0.01, ***p<0.001.

compared to the control (22,26-28). Rapamycin reduced the levels of p-mTOR, pERK1/2, and pTFEB and increased that of LAMP1 (29). Therefore, oxLDL inhibited the activation of TFEB via the ERK1/2/mTOR pathway, an effect reversed by the rapamycin-mediated inhibition of ERK1/2 and mTOR (**Fig. 1C**). Phospho-TFEB exists in the cytoplasm in an inactive state after phosphorylation by mTORC1 and ERK2. When dephosphorylated, TFEB translocates to the nucleus and, as a transcription factor, regulates lysosome biogenesis and autophagy. IF showed nuclear-cytoplasmic redistribution of TFEB in oxLDL-treated chondrocytes, indicating TFEB translocation from the nucleus to the cytoplasm. Cotreatment with rapamycin inhibited the oxLDL-induced nuclear export of TFEB. LysoSensor Green (DND-189) is a pH-dependent lysosomotropic pH probe. A decrease in LysoSensor Green fluorescence intensity indicates an alkaline shift in lysosomal pH. Cotreatment with

https://doi.org/10.4110/in.2024.24.e15

rapamycin and oxLDL rescued the alkaline shift in lysosomal pH caused by oxLDL alone. Therefore, inactivation of TFEB leads to a decline in lysosome function, an effect rescued by rapamycin (**Fig. 1D**).

oxLDL exacerbates necroptotic cell death in human OA chondrocytes

Autophagic flux is a measure of autophagic activity and includes the fusion and degradation of autophagosomes and lysosomes. Decreased autophagic flux leads to the accumulation of aggregated proteins, unnecessary proteins, and dysfunctional organelles, which are not cleared by autophagosomes or lysosomes. RIP3 and MLKL induce necroptosis and need to be degraded by autophagy. However, decreased autophagic flux results in the accumulation of RIP3 and MLKL, leading to excessive activation of necroptosis (30). Necroptosis is a type of programmed cell death mediated by the RIPK3 necrosome, which activates MLKL by phosphorylation. Western blotting showed increased levels of RIP3 and MLKL in oxLDL-treated chondrocytes, resulting in necroptosis (14,31). Cotreatment with rapamycin reduced the levels of these markers of necroptosis compared to oxLDL alone (**Fig. 2A**). IF showed increased signal intensities of RIP3 and pMLKL in oxLDL-treated chondrocytes, indicating necroptosis.

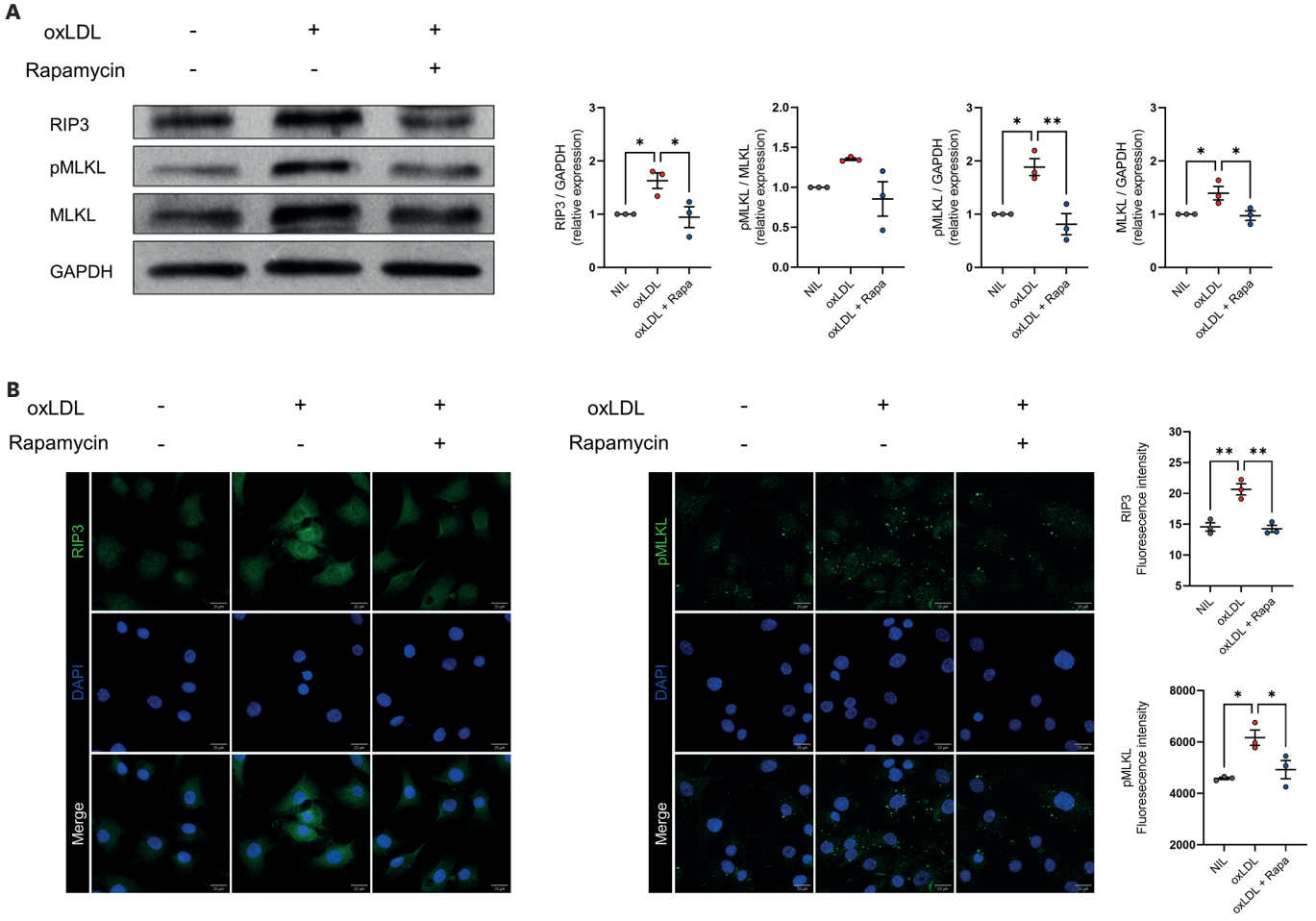

Figure 2. oxLDL induces necroptosis in human knee articular chondrocytes from patients with OA, an effect reversed by rapamycin. (A) Chondrocytes were stimulated with oxLDL (20 μg/mL) and rapamycin (100 nM) for 24 h, and the RIP3, pMLKL, MLKL, and GAPDH levels were analyzed by western blotting. (B) Chondrocytes from patients with OA were stimulated with oxLDL (20 μg/mL) and rapamycin (100 nM) for 24 h, and RIP3 and p-MLKL were detected by IF (magnification ×400). Data are means ± SEM; statistical significance was evaluated by the Bonferroni test.
*p<0.05, **p<0.01.

https://doi.org/10.4110/in.2024.24.e15

Cotreatment with rapamycin reduced the intensities of the IF signals of these markers compared to oxLDL alone. Therefore, necroptosis induced by oxLDL can be suppressed by activation of autophagy (**Fig. 2B**).

Dyslipidemia aggravates cartilage damage in mice with MIA-induced OA

MIA inhibits glycolysis and damages chondrocytes. Intra-articular injection of MIA increases chondrocyte death and proteoglycan depletion, resulting in the induction of OA. ApoE is a major protein component of LDL and very low-density lipoprotein (VLDL) that binds to the LDL receptor (LDLR) on cells, thereby facilitating the uptake of LDL into cells, and regulates the blood cholesterol level. ApoE deficiency increases the level of LDL in the blood, leading to dyslipidemia and CVDs (32). We investigated the effect of dyslipidemia on the pathogenesis of OA in mice with MIA-induced OA. Dyslipidemia was induced by feeding ApoE$^{-/-}$ mice a western diet for 5 wk; C57BL/6 mice, the background of ApoE$^{-/-}$ mice, were fed a normal chow diet (control). MIA (1 mg/kg) was intra-articularly injected into the right leg, and the pathogenesis of OA was examined (**Fig. 3A**). The LDL cholesterol level was increased in ApoE$^{-/-}$ mice fed a western diet compared to C57BL/6 mice fed a normal chow diet. Conversely, the HDL cholesterol level was decreased in ApoE$^{-/-}$ mice fed a western diet. These findings are consistent with the induction of dyslipidemia in ApoE$^{-/-}$ mice (**Fig. 3B**). The Mankin and Osteoarthritis Research Society International (OARSI) scores were increased in ApoE$^{-/-}$ mice fed a western diet compared to C57BL/6 mice fed a normal chow diet. This indicates that dyslipidemia exacerbates cartilage damage (15,16,33) (**Fig. 3C**). The *in vivo* histopathological findings were confirmed by IHC. IHC staining showed increased levels of IL-1β, IL-6, TNF-α (inflammatory cytokine), MMP13 (catabolic factor), LC3B, p62/SQSTM1 (autophagosome marker), RIP3, and pMLKL (necroptosis markers) in the cartilage tissue of MIA-induced OA mice with dyslipidemia compared to MIA-induced OA mice without dyslipidemia (34). Our findings suggest that dyslipidemia triggers abnormal autophagy and increases inflammatory cell death, thereby exacerbating OA (**Fig. 3D**).

Dyslipidemia exacerbates cartilage damage in mice with DMM surgery-induced OA

We investigated the effect of dyslipidemia on the pathogenesis of OA in a DMM surgery-induced OA model. To mimic injury-induced OA, we performed DMM surgery to induce OA and examined the effect of dyslipidemia on its pathogenesis. ApoE$^{-/-}$ mice were fed a western diet for 9 wk to induce hyperlipidemia; C57BL/6 mice were fed a normal chow diet (control). DMM surgery was performed on the right legs to induce OA, and the effect of dyslipidemia on its pathogenesis was evaluated (**Fig. 4A**). The LDL cholesterol level was increased in DMM-surgery mice fed a western diet compared to C57BL/6 mice fed a normal chow diet. Conversely, the HDL cholesterol level was decreased in DMM surgery mice fed a western diet. These findings are consistent with the induction of dyslipidemia in DMM-surgery mice (**Fig. 4B**). The weight increase was smaller in ApoE$^{-/-}$ mice with versus without dyslipidemia. This suggests that dyslipidemia is unlikely to induce OA via mechanical stress caused by weight change (**Fig. 4C**). In the von Frey hair assessment test, the PWT showed that DMM surgery mice with dyslipidemia had lower pain scores compared to DMM surgery mice without dyslipidemia. Therefore, severe dyslipidemia can exacerbate pain (**Fig. 4D**). The structural integrity of the articular cartilage was evaluated by Safranin O/Fast Green staining. Cartilage damage was exacerbated in DMM surgery mice with versus without dyslipidemia. The Mankin and OARSI scores were increased in DMM surgery mice with hyperlipidemia, indicating aggravation of OA (15,16,33) (**Fig. 4E**). IF staining showed that TFEB nuclear export was increased in chondrocytes from the articular cartilage of DMM surgery mice

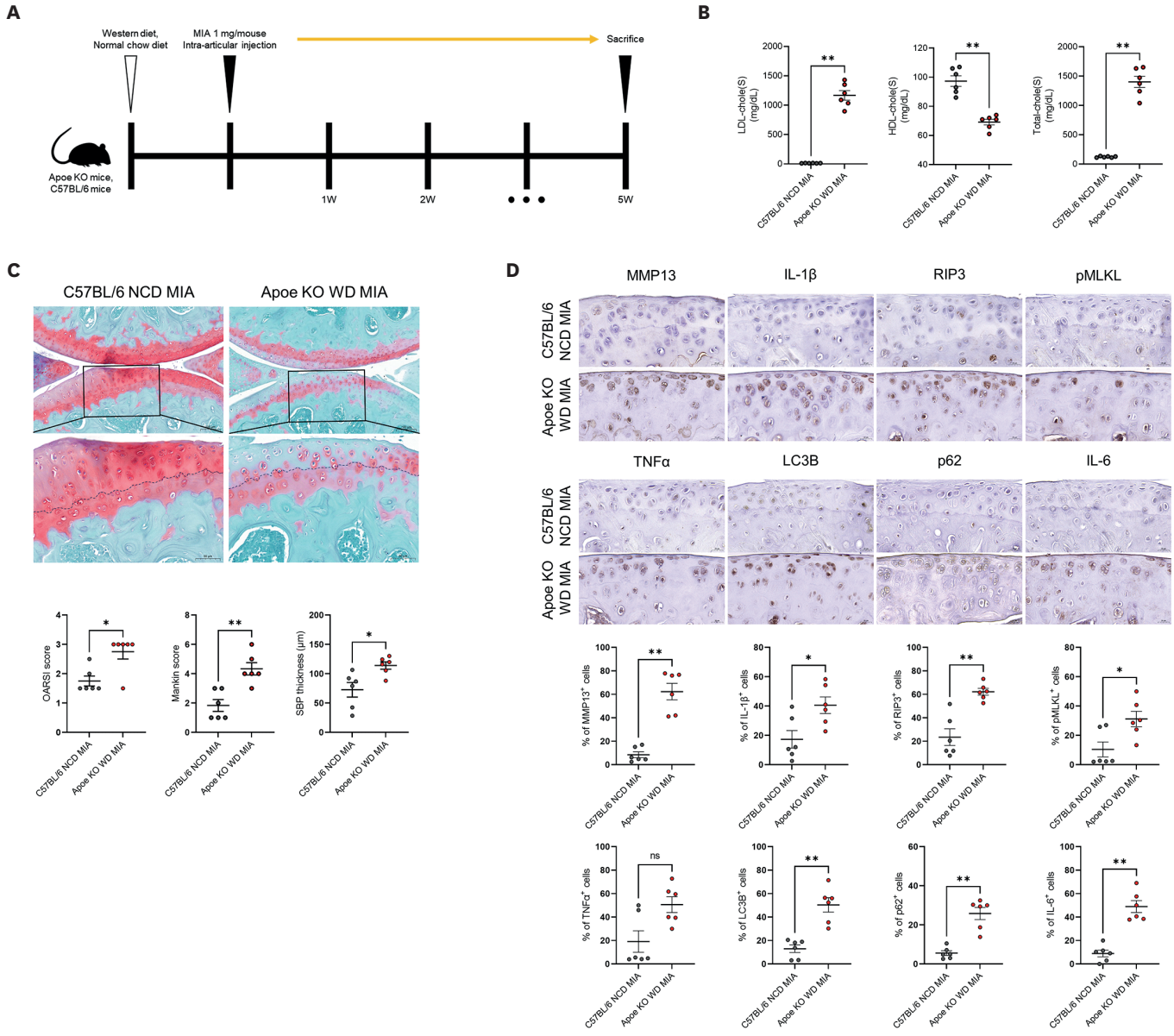

Figure 3. In the MIA-induced OA model, ApoE$^{-/-}$ mice fed a western diet had an increased LDL level and more severe OA compared with C57BL/6 mice fed a normal chow diet. (A) Diagram of the *in vivo* experiments (n=6 per group). (B) Serum levels of total cholesterol, LDL, and HDL of C57BL/6 mice fed a normal chow diet and ApoE$^{-/-}$ mice fed a western diet. (C) Mouse joint tissue was stained with Safranin O/Fast Green, and the Mankin and OARSI scores were obtained. Representative histological features are shown (magnifications ×200, ×500). (D) Mouse cartilage tissue was subjected to IHC (LC3B, p62/SQSTM1, RIP3, p-MLKL, MLKL, MMP13, and IL-1β) (magnification ×750).
Data are mean ± SEM; statistical significance was evaluated by the Mann–Whitney test and unpaired *t*-test.
ns, not significant.
*p<0.05, **p<0.01.

with versus without dyslipidemia. Therefore, severe dyslipidemia can induce TFEB nuclear export in chondrocytes (**Fig. 4F**). The *in vivo* histopathological findings were confirmed by IHC. IHC staining showed increased levels of IL-1β, IL-6, TNF-α (inflammatory cytokine), MMP13 (catabolic factor), LC3B, p62/SQSTM1 (autophagosome marker), RIP3, and pMLKL (necroptosis markers) in the cartilage tissue of DMM-surgery mice with versus without dyslipidemia (34). Therefore, dyslipidemia aggravates OA by triggering abnormal autophagic flux and inducing inflammatory cell death, consistent with the results of the mouse model of DMM surgery-induced OA (**Fig. 4G**).

https://doi.org/10.4110/in.2024.24.e15

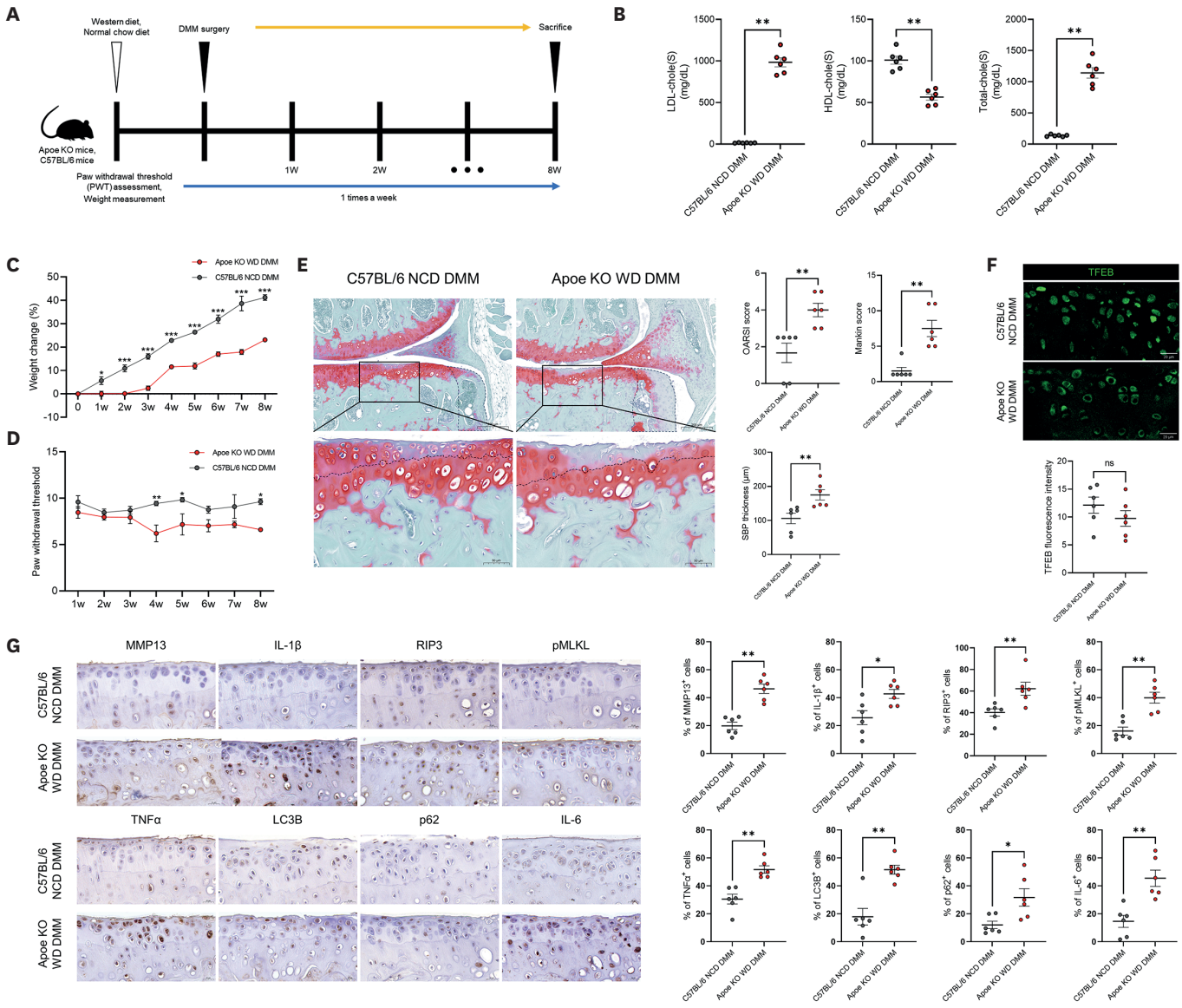

Figure 4. In the DMM surgery-induced OA model, ApoE$^{-/-}$ mice fed a western diet had an increased LDL level and more severe OA compared with C57BL/6 mice fed a normal chow diet. (A) Diagram of the *in vivo* experiments (n=6 per group). (B) Serum levels of total cholesterol, LDL-cholesterol, and HDL-cholesterol of C57BL/6 mice fed a normal chow diet and ApoE$^{-/-}$ mice fed a western diet. (C) Weight change of C57BL/6 mice fed a normal chow diet and ApoE$^{-/-}$ mice fed a western diet. (D) PWT in C57BL/6 mice fed a normal chow diet and ApoE$^{-/-}$ mice fed a western diet. (E) Mouse joint tissue was stained with Safranin O/Fast Green, and the Mankin and OARSI scores were evaluated. Representative histological features are shown (magnifications ×150, ×500). (F) TFEB nuclear translocation was observed in mouse articular-tissue chondrocytes by IF (magnification ×400). (G) Mouse cartilage tissue was subjected to IHC (LC3B, p62/SQSTM1, RIP3, p-MLKL, MLKL, MMP13, and IL-1β) (magnification ×750).
Data are mean ± SEM; statistical significance was evaluated by the Mann–Whitney test and unpaired *t*-test.
ns, not significant.
*p<0.05, **p<0.01.

Rosuvastatin and rapamycin suppress cartilage destruction in DMM surgery-induced OA mice

oxLDL impairs autophagic flux and induces necroptosis in endothelial cells and macrophages, making it a key initial risk factor for CVD. Therefore, reducing the LDL level is important for the treatment of dyslipidemia and CVD. Rosuvastatin is an HMG-CoA reductase inhibitor that suppresses cholesterol production in the liver, leading to a decrease in the LDL level and an increase in LDLR expression, in turn promoting the clearance of LDL from the bloodstream.

https://doi.org/10.4110/in.2024.24.e15

Rapamycin is an mTOR inhibitor that also inhibits ERK1/2, thereby increasing autophagic flux. ApoE$^{-/-}$ mice were fed a western diet for 9 wk to induce hyperlipidemia and underwent DMM surgery 1 week later to induce OA. Rosuvastatin (10 mg/kg) was administered orally daily from 1 wk (35,36) after DMM surgery, and 2 mg/kg rapamycin was administered intraperitoneally thrice weekly from 1 wk after DMM surgery (**Fig. 5A**). The weight change after drug administration was not significantly different between the groups. This suggests that the mechanical stress caused by drug administration did not affect OA pathogenesis (**Fig. 5B**). In the von Frey hair assessment test, the PWT showed recovery of pain scores

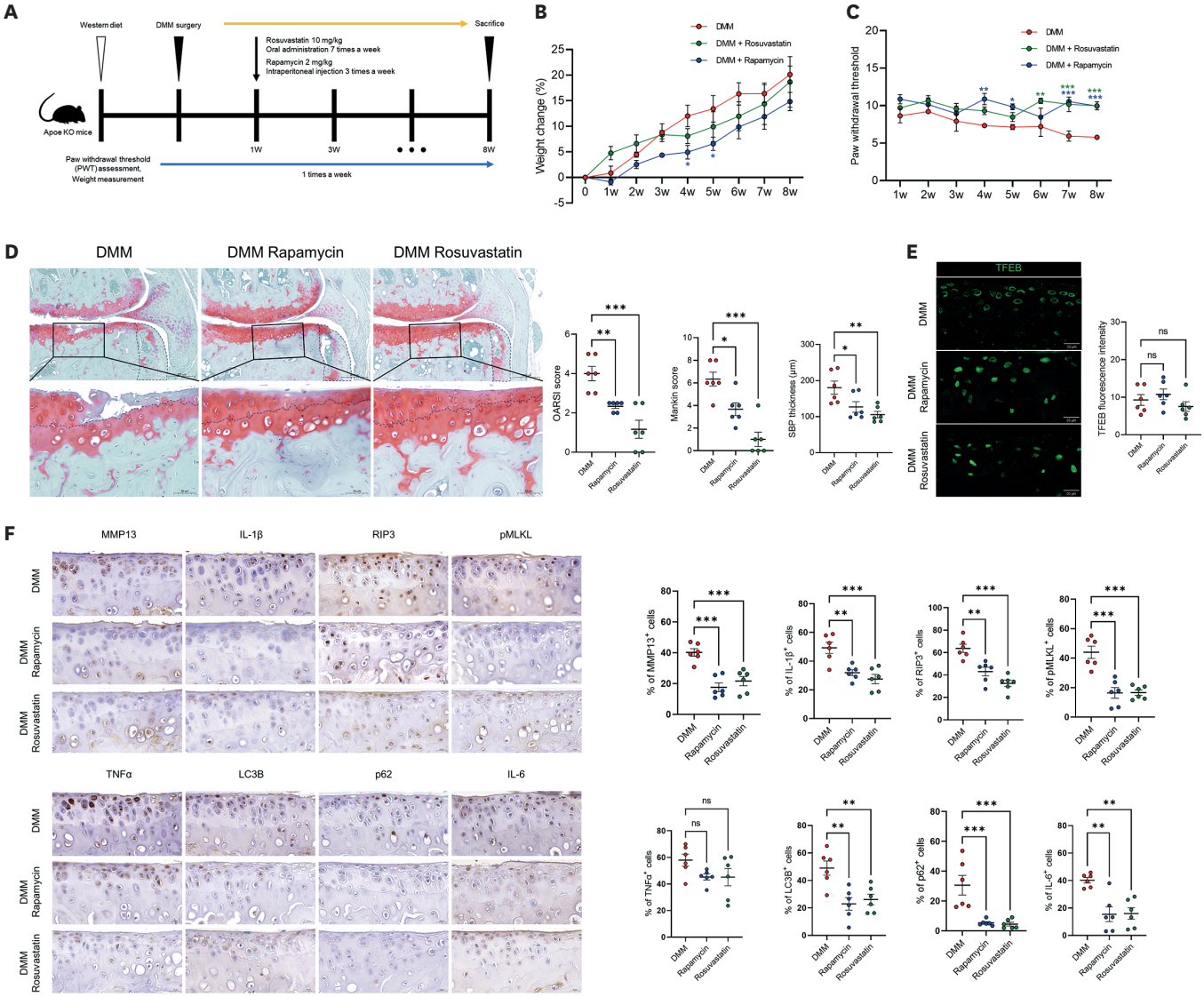

Figure 5. Rapamycin and rosuvastatin reduce OA severity in ApoE$^{-/-}$ mice fed a western diet. (A) Diagram of the *in vivo* experiments (n=6 mice per group). (B) Weight change in ApoE$^{-/-}$ mice fed a western diet and ApoE$^{-/-}$ mice fed a western diet administered with rapamycin and ApoE$^{-/-}$ mice fed a western diet administered with rosuvastatin. (C) PWT in C57BL/6 mice fed a normal chow diet and ApoE$^{-/-}$ mice fed a western diet. (D) Mouse joint tissue was stained with Safranin O/Fast Green, and the Mankin and OARSI scores were obtained. Representative histological features are shown (magnification ×150, ×500). (E) TFEB nuclear translocation was observed by IF in mouse articular tissue chondrocytes (magnification ×400). (F) Mouse cartialge tissue was subjected to IHC (LC3B, p62/SQSTM1, RIP3, p-MLKL, MLKL, MMP13, and IL-1β).
Data are mean ± SEM; statistical significance was evaluated by the Bonferroni test.
ns, not significant.
**p<0.01, ***p<0.001.

https://doi.org/10.4110/in.2024.24.e15

in mice treated with rapamycin and rosuvastatin relative to those that were untreated. Therefore, reducing the LDL level and inhibiting mTOR can alleviate pain (**Fig. 5C**). Safranin O/Fast Green staining showed that cartilage damage was alleviated in mice treated with rapamycin and rosuvastatin. The Mankin and OARSI scores indicated suppression of OA in mice treated with rapamycin and rosuvastatin (**Fig. 5D**) (37,38). IF for TFEB showed that mice treated with rosuvastatin and rapamycin had reduced TFEB nuclear export compared to untreated mice. Therefore, rosuvastatin and rapamycin can increase TFEB activity in chondrocytes (**Fig. 5E**). The *in vivo* histopathological findings were confirmed by IHC. IHC staining showed decreased levels of IL-1β, IL-6, TNF-α (inflammatory cytokine), MMP13 (catabolic factor), LC3B, p62/SQSTM1 (autophagosome marker), RIP3, and pMLKL (necroptosis markers) in the cartilage tissue of mice treated with rosuvastatin and rapamycin. Therefore, treatment with both rosuvastatin and rapamycin inhibited the dyslipidemia-induced abnormal autophagic flux and decreased necroptosis, thereby suppressing OA (**Fig. 5F**).

Dyslipidemia inhibited the autophagic flux and increased necroptosis in human OA cartilage

In a meta-analysis, 38.4% of patients with OA had concurrent CVD, which was markedly higher than the rate in the control cohort (9%) (39). This suggests a synergistic interaction among hyperlipidemia, OA and CVD. IHC staining of cartilage tissues from OA patients with dyslipidemia showed increased accumulation of autophagosomes (as indicated by an increased LC3B and p62/SQSTM1 level), as well as increased levels of RIP3 and p-MLKL (markers of necroptosis). These results suggest that dyslipidemia aggravates OA by impairing the autophagic flux and inducing necroptotic cell death (**Fig. 6**).

We next analyzed the correlations of OA with the levels of three types of lipids in patients with and without OA. We investigated the levels of triglycerides (TG), LDL, HDL, and TC of 304 patients without OA and 239 with OA who underwent total knee replacement arthroplasty (TKRA) and were enrolled from January 2016 to July 2023 (**Table 1**). The patients with OA

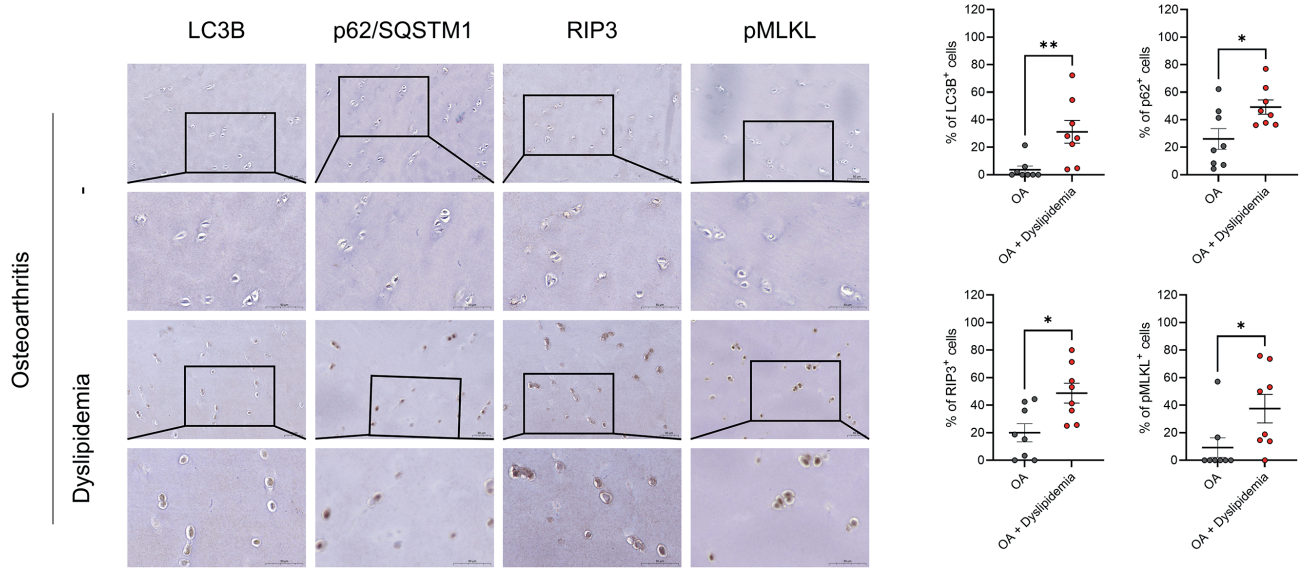

Figure 6. Reduced autophagic flux and increased apoptosis in the cartilage of patients with OA and dyslipidemia. Cartilage tissue from patients with OA with and without dyslipidemia was subjected to IHC (LC3B, p62/SQSTM1, RIP3, p-MLKL) (magnifications ×400, ×800).
Data are mean ± SEM; statistical significance was evaluated by the Mann–Whitney test and unpaired *t*-test.
*p<0.05, **p<0.01.

https://doi.org/10.4110/in.2024.24.e15

Table 1. Comparison of General characteristics between OA and non-OA groups

Variables	Category	OA (n=239)	Non-OA (n=304)	*t* or χ^2	p-value
Age (yr)		70.87±6.97	67.45±6.24	−6.01	<0.001
Sex	Male	35 (14.6)	141 (46.4)	61.52	<0.001
	Female	204 (85.4)	163 (53.6)		
Weight (kg)		64.75±12.17	63.23±9.57	−1.63	0.104
Height (m)		1.55±0.08	1.62±0.08	10.44	<0.001
Body mass index (kg/m^2)		26.89±4.26	23.99±2.95	−8.99	<0.001
Glucose (mg/dL)		120.88±39.24	114.23±38.79	−1.97	0.049
	>99	71 (29.7)	107 (35.2)	1.83	0.176
	≤99	168 (70.3)	197 (64.8)		
TC (mg/dL)		178.00±41.67	147.84±39.80	−8.58	<0.001
	≥200	73 (30.5)	32 (10.5)	34.37	<0.001
	<200	166 (69.5)	272 (89.5)		
TG (mg/dL)		157.90±118.94	113.91±45.18	−5.42	<0.001
	≥150	97 (40.6)	55 (18.1)	33.59	<0.001
	<150	142 (59.4)	249 (81.9)		
LDL (mg/dL)		108.64±87.95	89.27±28.09	−3.28	0.001
	≥150	27 (11.3)	8 (2.6)	16.66	<0.001
	<150	212 (88.7)	296 (97.4)		
HDL (mg/dL)		54.33±13.78	50.12±12.81	−3.67	<0.001
	≤40	28 (11.9)	57 (18.8)	4.75	0.029
	>40	208 (88.1)	247 (81.2)		

Values are presented as mean ± SD for continuous variables and frequency (%) for categorical variables.

had a higher average age (70.87±6.97 years) than those without OA (67.45±6.24 years), and the proportions of males were 14.6% and 46.4%, respectively (p<0.001). Although the between-group difference in body weight was not significant, patients with OA had a lower average height (155 and 162 cm, respectively) and a significantly higher body mass index (26.89±4.26 and 23.99±2.95 kg/m^2, respectively) than those without OA (p<0.001). There was no significant difference in blood glucose level between the patients with and without OA. The patients with OA had significantly higher levels of TG, LDL, and TC than those without OA (all p≤0.001). The HDL level was significantly lower in the patients with than in those without OA (p≤0.029). The proportions of patients with OA who had abnormal lipid levels were 11.3% for LDL, 30.5% for TC, and 40.6% for TG. Among the patients without OA, the corresponding values were 2.6% for LDL, 10.5% for TC, and 18.1% for TG. The general characteristics of the 239 patients who underwent TKRA are listed in **Table 2**. The patients

Table 2. General characteristics (n=239)

Characteristics	Categories	Mean ± SD or No. (%)	Max	Min
Age (yr)		70.87±6.97	49	86
Sex	Female	204 (85.4)		
Medication				
Statin		93 (38.9)		
Omega-3		84 (35.1)		
Metformin		38 (15.9)		
Insulin		18 (7.5)		
CCOX		176 (73.6)		
Glucose		120.88±39.24	76	341
Post-operative CRP (mg/dL)		7.76±5.60	0.48	24.26
Duration for normal CRP value (days)		18.54±9.56	4	66
Body mass index (kg/m^2)		26.89±4.26	16.33	54.68
Underlying disease				
Diabetes mellitus		68 (28.5)		
Hypertension		146 (61.1)		
Dyslipidemia		84 (35.1)		
Stroke		17 (7.1)		

CCOX, cytochrome c oxidase.

https://doi.org/10.4110/in.2024.24.e15

Table 3. Comparison of post-operative CRP levels according to dyslipidemia group

Variables	TC		TG		LDL	
	≥200 (n=73)	<200 (n=166)	≥150 (n=97)	<150 (n=142)	≥150 (n=27)	<150 (n=212)
Post-operative CRP levels	9.13±6.21	7.16±5.21	9.36±6.14	6.67±4.92	10.34±6.55	7.43±5.39
t (p)	−2.38 (0.019)		−3.61 (<0.001)		−2.58 (0.011)	

Values are presented as mean ± SD.

with dyslipidemia had a significantly higher C-reactive protein (CRP) level 3 h after TKRA (p<0.001–0.019). The CRP, LDL (10.34±6.55), TG (9.36±6.14), and TC (9.13±6.21) elevations are listed in **Table 3**.

DISCUSSION

OA is linked to obesity: one-third of older adults with obesity have OA. The inflammatory responses triggered by the metabolic syndrome are also linked to OA. However, research on the mechanisms underlying the link between OA and the metabolic syndrome is lacking.

Chondrocytes treated with oxLDL have decreased viability and increased senescence (12,14,40), and oxLDL promotes cartilage degradation by increasing the expression of MCP-1 (41). Aging could be important in the pathogenesis of OA because autophagy decreases with age. The expression of autophagy-related proteins in articular cartilage decreases with age in human and mouse. Therefore, modulation of autophagy may serve as a therapeutic strategy to slow the progression of OA (19). If so, the increased oxLDL level in patients with OA may decrease cell viability, increase the MCP-1 level, and inactivate autophagy, thereby triggering inflammatory cell death.

We investigated the effect of an elevated oxLDL level on the chondrocytes of patients with OA. Treatment of such chondrocytes with oxLDL increased the p62/SQSTM1 level and inhibited the activity of TFEB, thereby decreasing the autophagic flux and leading to autophagic dysfunction and necroptosis. TFEB is phosphorylated by mTORC1 and ERK2 and exists in an inactive state in the cytoplasm. Upon dephosphorylation, TFEB translocates to the nucleus and, as a transcription factor, regulates lysosomal biosynthesis and autophagy. oxLDL inhibited the activity of TFEB, leading to lysosomal dysfunction, but treatment with rapamycin, an inhibitor of mTORC, restored TFEB activity and normal autophagy. These results suggest that OA can be exacerbated by an elevated oxLDL level (**Fig. 7**).

The levels of TG, LDL, and TC were significantly increased in patients with OA. These results suggest an inflammatory response to cartilage, synovial membranes, and surrounding tissues in such patients (34) (42), which may contribute to their sensitivity to external stimuli. The progression of OA is associated with inflammation and oxidative stress, as indicated by a significantly elevated blood level of CRP (43). Therefore, the incidence of OA may be lower among patients on a low-LDL diet. The expression of CRP is increased in ApoE KO mice (44).

The levels of LDL and CRP are high in patients with early-stage OA (45). A limitation of this study was that, in the dyslipidemia group, the relative contributions of LDL, TG, and TC to OA were not determined, and a meta-analysis encompassing other causes of OA is needed. In addition, it is necessary to analyze whether blood CRP and cytokine levels are significantly reduced in patients with OA on an LDL diet. Furthermore, there is a need to obtain visual

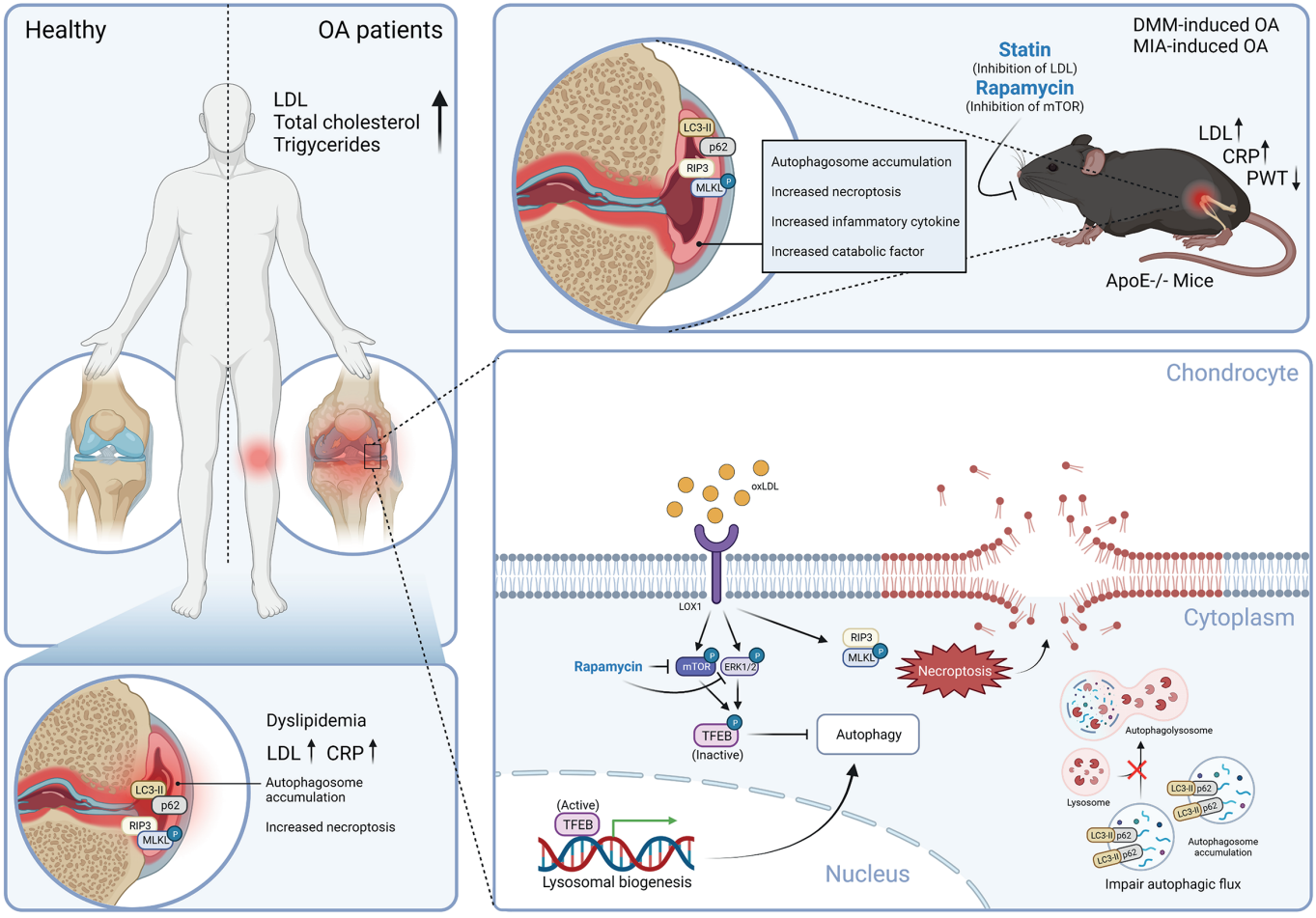

Figure 7. oxLDL activates ERK1/2 and mTOR, leading to inactivation of TFEB and inhibition of autophagic flux, thereby inducing necroptosis (graphic created with BioRender.com).

analog scale, Western Ontario and McMaster Universities Arthritis Index, and satisfaction data from patients with well-controlled dyslipidemia who are scheduled to undergo TKRA.

Autophagy plays a critical role in chondrocyte metabolism. Autophagy can repair damage, inhibit aging, and suppress the pathogenesis of degenerative arthritis. Although great strides have been made, there remain gaps in our understanding of the roles of autophagy and chondrocyte metabolism in OA. In this study, oxLDL, which is implicated in dyslipidemia, inhibited the activity of TFEB in chondrocytes, reduced autophagic flux, and induced necroptosis. Indeed, it accelerated the development of OA in 2 mouse models by causing abnormal autophagic flux and inducing inflammatory cell death. Treatment with rapamycin, which activates TFEB, significantly reduced cartilage damage, ameliorating the progression of OA and exerting anti-nociceptive and chondroprotective effects. Our findings suggest a role for TFEB in the pathogenesis of dyslipidemia-induced OA; therefore, TFEB has potential as a therapeutic target for OA.

https://doi.org/10.4110/in.2024.24.e15

ACKNOWLEDGEMENTS

This research was supported by the National Research Foundation of Korea grant funded by the Korea government (grant No. 2023R1A2C2003846). This research was supported by a grant of the Korea Health Technology R&D Project through the Korea Health Industry Development Institute, funded by the Ministry of Health & Welfare, Republic of Korea (grant No. HV22C0069).

REFERENCES

1. Hashimoto K, Akagi M. The role of oxidation of low-density lipids in pathogenesis of osteoarthritis: a narrative review. *J Int Med Res* 2020;48:300060520931609. PUBMED | CROSSREF
2. de Munter W, Blom AB, Helsen MM, Walgreen B, van der Kraan PM, Joosten LA, van den Berg WB, van Lent PL. Cholesterol accumulation caused by low density lipoprotein receptor deficiency or a cholesterol-rich diet results in ectopic bone formation during experimental osteoarthritis. *Arthritis Res Ther* 2013;15:R178. PUBMED | CROSSREF
3. Akkiraju H, Nohe A. Role of chondrocytes in cartilage formation, progression of osteoarthritis and cartilage regeneration. *J Dev Biol* 2015;3:177-192. PUBMED | CROSSREF
4. Rellmann Y, Eidhof E, Dreier R. Review: ER stress-induced cell death in osteoarthritic cartilage. *Cell Signal* 2021;78:109880. PUBMED | CROSSREF
5. Dai W, Cheng J, Leng X, Hu X, Ao Y. The potential role of necroptosis in clinical diseases (review). *Int J Mol Med* 2021;47:1-16. PUBMED | CROSSREF
6. Duan R, Xie H, Liu ZZ. The role of autophagy in osteoarthritis. *Front Cell Dev Biol* 2020;8:608388. PUBMED | CROSSREF
7. Funck-Brentano T, Nethander M, Movérare-Skrtic S, Richette P, Ohlsson C. Causal factors for knee, hip, and hand osteoarthritis: a Mendelian randomization study in the UK Biobank. *Arthritis Rheumatol* 2019;71:1634-1641. PUBMED | CROSSREF
8. Linton MF, Yancey PG, Davies SS, Jerome WG, Linton EF, Song WL, Doran AC, Vickers KC. The role of lipids and lipoproteins in atherosclerosis. In: Feingold KR, Anawalt B, Blackman MR, Boyce A, Chrousos G, Corpas E, de Herder WW, Dhatariya K, Dungan K, Hofland J, et al., editors. Endotext. South Dartmouth, MA: MDText.com, Inc.; 2000.
9. Nemet M, Blazin T, Milutinovic S, Cebovic T, Stanojevic D, Zvekic Svorcan J. Association between metabolic syndrome, its components, and knee osteoarthritis in premenopausal and menopausal women: a pilot study. *Cureus* 2022;14:e26726. PUBMED | CROSSREF
10. Fang Z, Li X, Wang S, Jiang Q, Loor JJ, Jiang X, Ju L, Yu H, Shen T, Chen M, et al. Overactivation of hepatic mechanistic target of rapamycin kinase complex 1 (mTORC1) is associated with low transcriptional activity of transcription factor EB and lysosomal dysfunction in dairy cows with clinical ketosis. *J Dairy Sci* 2022;105:4520-4533. PUBMED | CROSSREF
11. Schwager JL, Nevitt MC, Torner J, Lewis CE, Matthan NR, Wang N, Sun X, Lichtenstein AH, Felson D; Multicenter Osteoarthritis Study Group. Association of serum low-density lipoprotein, high-density lipoprotein, and total cholesterol with development of knee osteoarthritis. *Arthritis Care Res (Hoboken)* 2022;74:274-280. PUBMED | CROSSREF
12. Nakagawa T, Yasuda T, Hoshikawa H, Shimizu M, Kakinuma T, Chen M, Masaki T, Nakamura T, Sawamura T. LOX-1 expressed in cultured rat chondrocytes mediates oxidized LDL-induced cell death-possible role of dephosphorylation of Akt. *Biochem Biophys Res Commun* 2002;299:91-97. PUBMED | CROSSREF
13. Hashimoto K, Oda Y, Nakamura F, Kakinoki R, Akagi M. Lectin-like, oxidized low-density lipoprotein receptor-1-deficient mice show resistance to age-related knee osteoarthritis. *Eur J Histochem* 2017;61:2762. PUBMED | CROSSREF
14. Akagi M, Kanata S, Mori S, Itabe H, Sawamura T, Hamanishi C. Possible involvement of the oxidized low-density lipoprotein/lectin-like oxidized low-density lipoprotein receptor-1 system in pathogenesis and progression of human osteoarthritis. *Osteoarthritis Cartilage* 2007;15:281-290. PUBMED | CROSSREF
15. Cao C, Shi Y, Zhang X, Li Q, Zhang J, Zhao F, Meng Q, Dai W, Liu Z, Yan W, et al. Cholesterol-induced LRP3 downregulation promotes cartilage degeneration in osteoarthritis by targeting Syndecan-4. *Nat Commun* 2022;13:7139. PUBMED | CROSSREF

16. Choi WS, Lee G, Song WH, Koh JT, Yang J, Kwak JS, Kim HE, Kim SK, Son YO, Nam H, et al. The CH25H-CYP7B1-RORα axis of cholesterol metabolism regulates osteoarthritis. *Nature* 2019;566:254-258. PUBMED | CROSSREF
17. Shen P, Zhu Y, Zhu L, Weng F, Li X, Xu Y. Oxidized low density lipoprotein facilitates tumor necrosis factor-α mediated chondrocyte death via autophagy pathway. *Mol Med Rep* 2017;16:9449-9456. PUBMED | CROSSREF
18. Luo P, Gao F, Niu D, Sun X, Song Q, Guo C, Liang Y, Sun W. The role of autophagy in chondrocyte metabolism and osteoarthritis: a comprehensive research review. *BioMed Res Int* 2019;2019:5171602. PUBMED | CROSSREF
19. Caramés B, Taniguchi N, Otsuki S, Blanco FJ, Lotz M. Autophagy is a protective mechanism in normal cartilage, and its aging-related loss is linked with cell death and osteoarthritis. *Arthritis Rheum* 2010;62:791-801. PUBMED | CROSSREF
20. Sun K, Guo Z, Zhang J, Hou L, Liang S, Lu F, Wang G, Xu J, Zhang X, Guo F, et al. Inhibition of TRADD ameliorates chondrocyte necroptosis and osteoarthritis by blocking RIPK1-TAK1 pathway and restoring autophagy. *Cell Death Dis* 2023;9:109. PUBMED | CROSSREF
21. Zhang H, Ge S, Ni B, He K, Zhu P, Wu X, Shao Y. Augmenting ATG14 alleviates atherosclerosis and inhibits inflammation via promotion of autophagosome-lysosome fusion in macrophages. *Autophagy* 2021;17:4218-4230. PUBMED | CROSSREF
22. Qin X, He W, Yang R, Liu L, Zhang Y, Li L, Si J, Li X, Ma K. Inhibition of Connexin 43 reverses ox-LDL-mediated inhibition of autophagy in VSMC by inhibiting the PI3K/Akt/mTOR signaling pathway. *PeerJ* 2022;10:e12969. PUBMED | CROSSREF
23. Zhang Q, Cao S, Qiu F, Kang N. Incomplete autophagy: trouble is a friend. *Med Res Rev* 2022;42:1545-1587. PUBMED | CROSSREF
24. Martina JA, Chen Y, Gucek M, Puertollano R. MTORC1 functions as a transcriptional regulator of autophagy by preventing nuclear transport of TFEB. *Autophagy* 2012;8:903-914. PUBMED | CROSSREF
25. Tan A, Prasad R, Lee C, Jho EH. Past, present, and future perspectives of transcription factor EB (TFEB): mechanisms of regulation and association with disease. *Cell Death Differ* 2022;29:1433-1449. PUBMED | CROSSREF
26. Akhmedov A, Camici GG, Reiner MF, Bonetti NR, Costantino S, Holy EW, Spescha RD, Stivala S, Schaub Clerigué A, Speer T, et al. Endothelial LOX-1 activation differentially regulates arterial thrombus formation depending on oxLDL levels: role of the Oct-1/SIRT1 and ERK1/2 pathways. *Cardiovasc Res* 2017;113:498-507. PUBMED | CROSSREF
27. Zhang Z, Yue P, Lu T, Wang Y, Wei Y, Wei X. Role of lysosomes in physiological activities, diseases, and therapy. *J Hematol Oncol* 2021;14:79. PUBMED | CROSSREF
28. Tao J, Yang P, Xie L, Pu Y, Guo J, Jiao J, Sun L, Lu D. Gastrodin induces lysosomal biogenesis and autophagy to prevent the formation of foam cells via AMPK-FoxO1-TFEB signalling axis. *J Cell Mol Med* 2021;25:5769-5781. PUBMED | CROSSREF
29. Zhou YD, Cao XQ, Liu ZH, Cao YJ, Liu CF, Zhang YL, Xie Y. Rapamycin inhibits oxidized low density lipoprotein uptake in human umbilical vein endothelial cells via mTOR/NF-κB/LOX-1 pathway. *PLoS One* 2016;11:e0146777. PUBMED | CROSSREF
30. Xu C, Wu J, Wu Y, Ren Z, Yao Y, Chen G, Fang EF, Noh JH, Liu YU, Wei L, et al. TNF-α-dependent neuronal necroptosis regulated in Alzheimer's disease by coordination of RIPK1-p62 complex with autophagic UVRAG. *Theranostics* 2021;11:9452-9469. PUBMED | CROSSREF
31. Karunakaran D, Geoffrion M, Wei L, Gan W, Richards L, Shangari P, DeKemp EM, Beanlands RA, Perisic L, Maegdefessel L, et al. Targeting macrophage necroptosis for therapeutic and diagnostic interventions in atherosclerosis. *Sci Adv* 2016;2:e1600224. PUBMED | CROSSREF
32. Steinl DC, Kaufmann BA. Ultrasound imaging for risk assessment in atherosclerosis. *Int J Mol Sci* 2015;16:9749-9769. PUBMED | CROSSREF
33. Hashimoto K, Mori S, Oda Y, Nakano A, Sawamura T, Akagi M. Lectin-like oxidized low density lipoprotein receptor 1-deficient mice show resistance to instability-induced osteoarthritis. *Scand J Rheumatol* 2016;45:412-422. PUBMED | CROSSREF
34. de Munter W, van den Bosch MH, Slöetjes AW, Croce KJ, Vogl T, Roth J, Koenders MI, van de Loo FA, van den Berg WB, van der Kraan PM, et al. High LDL levels lead to increased synovial inflammation and accelerated ectopic bone formation during experimental osteoarthritis. *Osteoarthritis Cartilage* 2016;24:844-855. PUBMED | CROSSREF
35. Monetti M, Canavesi M, Camera M, Parente R, Paoletti R, Tremoli E, Corsini A, Bellosta S. Rosuvastatin displays anti-atherothrombotic and anti-inflammatory properties in ApoE-deficient mice. *Pharmacol Res* 2007;55:441-449. PUBMED | CROSSREF

36. Sironi L, Gianazza E, Gelosa P, Guerrini U, Nobili E, Gianella A, Cremonesi B, Paoletti R, Tremoli E. Rosuvastatin, but not simvastatin, provides end-organ protection in stroke-prone rats by antiinflammatory effects. *Arterioscler Thromb Vasc Biol* 2005;25:598-603. PUBMED | CROSSREF
37. Yudoh K, Karasawa R. Statin prevents chondrocyte aging and degeneration of articular cartilage in osteoarthritis (OA). *Aging (Albany NY)* 2010;2:990-998. PUBMED | CROSSREF
38. Caramés B, Hasegawa A, Taniguchi N, Miyaki S, Blanco FJ, Lotz M. Autophagy activation by rapamycin reduces severity of experimental osteoarthritis. *Ann Rheum Dis* 2012;71:575-581. PUBMED | CROSSREF
39. Hall AJ, Stubbs B, Mamas MA, Myint PK, Smith TO. Association between osteoarthritis and cardiovascular disease: systematic review and meta-analysis. *Eur J Prev Cardiol* 2016;23:938-946. PUBMED | CROSSREF
40. Zushi S, Akagi M, Kishimoto H, Teramura T, Sawamura T, Hamanishi C. Induction of bovine articular chondrocyte senescence with oxidized low-density lipoprotein through lectin-like oxidized low-density lipoprotein receptor 1. *Arthritis Rheum* 2009;60:3007-3016. PUBMED | CROSSREF
41. Akagi M, Ueda A, Teramura T, Kanata S, Sawamura T, Hamanishi C. Oxidized LDL binding to LOX-1 enhances MCP-1 expression in cultured human articular chondrocytes. *Osteoarthritis Cartilage* 2009;17:271-275. PUBMED | CROSSREF
42. Farnaghi S, Crawford R, Xiao Y, Prasadam I. Cholesterol metabolism in pathogenesis of osteoarthritis disease. *Int J Rheum Dis* 2017;20:131-140. PUBMED | CROSSREF
43. Jin X, Beguerie JR, Zhang W, Blizzard L, Otahal P, Jones G, Ding C. Circulating C reactive protein in osteoarthritis: a systematic review and meta-analysis. *Ann Rheum Dis* 2015;74:703-710. PUBMED | CROSSREF
44. Nie P, Yang F, Wan F, Jin S, Pu J. Analysis of microRNAs associated with carotid atherosclerotic plaque rupture with thrombosis. *Front Genet* 2021;12:599350. PUBMED | CROSSREF
45. Herrero-Manley L, Alabajos-Cea A, Suso-Martí L, Cuenca-Martínez F, Calatayud J, Casaña J, Viosca-Herrero E, Vázquez-Arce I, Ferrer-Sargues FJ, Blanco-Díaz M. Serum lipid biomarkers and inflammatory cytokines associated with onset and clinical status of patients with early knee osteoarthritis. *Front Nutr* 2023;10:1126796. PUBMED | CROSSREF